Systems & Control Transactions

Research Article
Foundations of Computer Aided Process Design (FOCAPD 2024)
Breckenridge, Colorado, USA. July 14-18, 2024
Peer Reviewed Conference Proceeding

PSE PRESS

NMPC for Mode-Switching Operation of Reversible Solid Oxide Cell Systems

Mingrui Li[e], Douglas A. Allan[ac], San Dinh[e], Lorenz T. Biegler[e], Debangsu Bhattacharyya[d], Vibhav Dabadghao[e], Nishant Giridhar[d], Stephen E. Zitney[b]*

[a] National Energy Technology Laboratory, Pittsburgh, PA 15236
[b] National Energy Technology Laboratory, Morgantown, WV 26507
[c] NETL Support Contractor, Pittsburgh, PA 15236
[d] West Virginia University, Morgantown, WV 26507
[e] Carnegie Mellon University, Pittsburgh, PA 15213
* Corresponding Author: steve.zitney@netl.doe.gov.

ABSTRACT

Solid oxide cells (SOCs) are a promising dual-mode technology that generates hydrogen through high-temperature water electrolysis and generates power through a fuel cell reaction that consumes hydrogen. Reversible operation of SOCs requires a transition between these two modes for hydrogen production setpoints as the demand and price of electricity fluctuate. Moreover, a well-functioning control system is important to avoid cell degradation during mode-switching operation. In this work, we apply nonlinear model predictive control (NMPC) to an SOC module and supporting equipment and compare NMPC performance to classical proportional integral (PI) control strategies, while ramping between the modes of hydrogen and power production. While both control methods provide similar performance in many metrics, NMPC significantly reduces cell thermal gradients and curvatures (mixed spatial-temporal partial derivatives) during mode switching. A dynamic process flowsheet of the reversible SOC system was developed in the open-source, equation-based IDAES modeling framework. Our IDAES dynamic simulation results show that NMPC can ramp the SOC system between hydrogen and power production targets within short mode-switching times. Moreover, NMPC can comply with operating limits in the SOC system more effectively than PI, and only NMPC can directly enforce user-specified limits for mixed spatial-temporal partial derivatives of temperature. This allows for management of the trade-off between operating efficiency and cell degradation, which is dependent on these temperature curvatures.

Keywords: Sustainability, Implementation, Energy & Environment, Process Optimization & Control, NMPC, Solid Oxide Cells, SOEC, SOFC

INTRODUCTION

In recent years, a growing share of variable renewable energy generation and ambitious decarbonization targets have spurred a notable shift away from fossil fuels, with hydrogen poised to play a crucial role in this energy transition. By combining hydrogen production and electricity generation, integrated energy systems based on reversible SOC technology (rSOC) can be optimized to provide the operational flexibility required to meet the varying load demand of the modern grid. Hydrogen can function as a valuable energy storage medium and as a versatile feedstock for other purposes. While most industrial hydrogen today is produced through steam methane reforming, which uses a fossil fuel feedstock, water electrolysis is a promising replacement, producing no direct greenhouse gas emissions when renewable energy is used.

For hydrogen production through water electrolysis, Nernst potential, the minimum potential difference at which electrolysis occurs, decreases with increasing reaction temperature. Because solid oxide electrolysis cells (SOECs) and solid oxide fuel cells (SOFCs) operate at 600°C to 1000°C, much higher temperatures than those

of other electrolysis technologies, they are good candidates for efficient water electrolysis. In power production mode, high temperature operation allows various fuels, including hydrogen, to rapidly undergo oxidation reaction on the fuel electrode. However, high temperature operation comes with significant drawbacks. Besides additional heat exchange equipment and good thermal insulation requirements, transitions between operating points must be carefully controlled to minimize power requirements and avoid thermal stress.

Many SOC systems are reversible and can operate as hydrogen fuel cells when grid demand becomes high. This flexible operation is necessary to stabilize the grid and operate profitably with intermittent renewable energy. Switching between SOEC and SOFC modes while considering both operating performance and equipment longevity can be challenging. Ferrari [1] coupled PI controllers with feed-forward approaches to reduce thermal gradients and limit the peak anode-cathode differential pressure for a tubular SOFC/GT hybrid system. However, modeling of the SOFC was based on "lumped volume" 0D models, and the chemical reactions were assumed to be at equilibrium. Abbaker et al. [2] used a discrete-time adaptive terminal sliding-mode control strategy for voltage setpoint tracking for an SOFC. A pseudo-partial derivative technique was used to model the SOFC. Botta et al. [3] considered an rSOFC system and applied a PI controller to prevent dangerous operating conditions at the stack level. They analyzed individual SOFC and SOEC modes, as well as switching between these modes during reversible operation of the stack. Spivey and Edgar [4] developed a dynamic model for a tubular SOFC to capture the dynamics of critical thermal stress drivers and applied it to a MIMO predictive controller. Schotman [5] applied an output feedback adaptive NMPC approach to an rSOC system to control cell temperature and temperature gradients while maintaining desired level of power output. Xing et al. [6] designed a model predictive control (MPC) strategy based on a linear parameter varying model to improve short-term tracking performance and long-term operating efficiency for an rSOC plant. The process model for rSOC was a linear state-space model of the plant.

SOC systems are good candidates for nonlinear MPC (NMPC) since many manipulated variables (MVs) are highly interactive. As mentioned earlier, NMPC [7-8] uses a system model to predict system response to a sequence of MVs and optimizes it with respect to performance metrics. Because the controller can manipulate several degrees of freedom, it affords a quicker response than that of classical control.

In this work, NMPC is applied to an SOC module and supporting equipment, with its performance compared to that of classical PI control strategies for switching between the modes of hydrogen and power production. Switching from maximum hydrogen production to power generation and back to hydrogen production is demonstrated for the SOC system. Performance is judged based on the speed of production rate transition, total power usage, and whether unsafe thermal levels occur in the SOC.

PROCESS MODELING

The SOC system flowsheet is built in the IDAES modeling framework [9]. The SOC model is publicly available in the IDAES GitHub repository [10], and a preliminary version is available in the literature [11]. There is ambiguity in denoting the cell “anode” and “cathode” in a reversible SOC, because the anode in fuel cell mode is the cathode in electrolysis mode and vice-versa. Hence, we refer to the electrode where hydrogen is produced or consumed as the fuel electrode and the electrode where oxygen is produced or consumed as the oxygen electrode. Model parameters were fit to data from the two-cell fuel electrode supported short stack shown in Figure 1 for the SOC system described in Figure 2.

The SOC model shown in Figure 1 is one dimensional in channels and (potentially) two dimensional in the fuel electrode, electrolyte, oxygen electrode, and interconnect. However, because the thickness of the positive electrode-electrolyte-negative electrode (PEN) assembly is only approximately one millimeter (with almost all of that in the fuel electrode), only one finite element is used in the x direction for the fuel electrode, while the electrolyte and oxygen electrode are approximated as thin-film resistors. The interconnect, which is 5 mm thick, also uses one finite element. The length of the cell in the z direction is 23.5 cm and ten finite elements are used in that direction for all subcomponents. The cell is run in a countercurrent configuration. The interconnect is represented by a periodic boundary condition, with one end attached to the top of the fuel channel and one to the bottom of the oxygen channel, to represent a cell in the center of a large stack. The cell model does not consider losses to the environment.

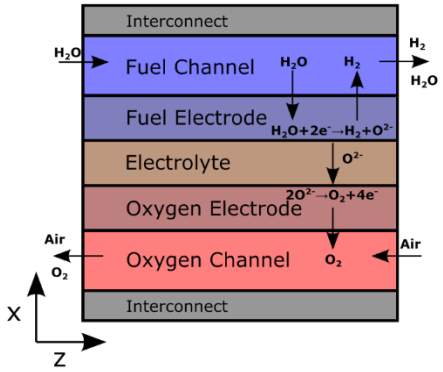

Figure 1. SOC configuration. Note that this diagram is not

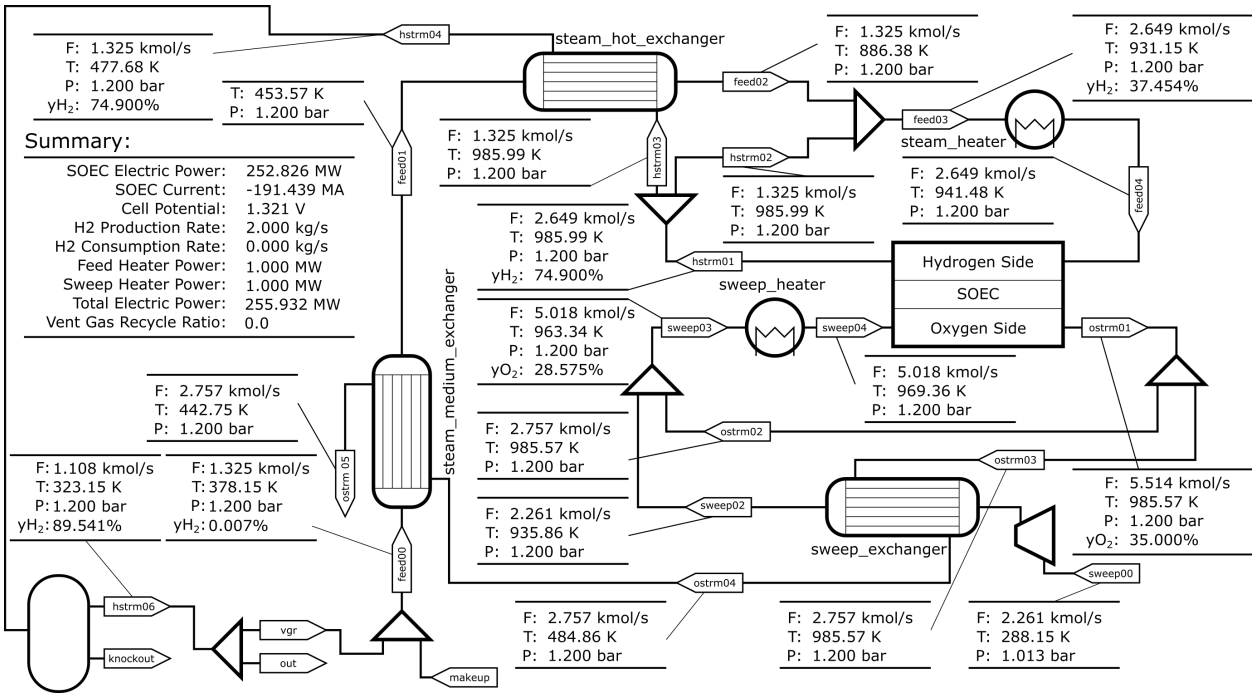

Figure 2. SOC system flowsheet in SOEC mode.

to scale—the cell is millimeters thick, and the electrolyte and oxygen electrode are micrometers thick.

The SOC system flowsheet in Figure 2 consists of supporting equipment for the SOC module. Three cross-flow heat exchangers heat incoming air and water/hydrogen up to the cell's operating temperature of approximately 975 K (in electrolysis mode). Two resistive trim heaters provide additional heat as well as control the temperature of the inlet streams to the stack. The oxygen stream is vented to the atmosphere, while the fuel stream goes to a condenser. Water is knocked out in a flash vessel. The hydrogen-rich gas exiting the flash is either mixed with the fresh fuel inlet to return to the SOC (in fuel-cell mode) or is taken out of the system for compression and further purification (in electrolysis mode). The heat exchangers and trim heaters use 1D models, whereas the other supporting equipment units use 0D models. Because of the short gas phase residence time in the system (about four seconds for the fuel side in electrolysis mode), gas phase holdups are turned off in all units, leaving thermal holdups as the primary source of dynamic behavior. For every discretized time step within the dynamic model, the SOC system flowsheet consists of 900 differential equations, 6955 algebraic equations, and 4311 inequalities.

In electrolysis mode, the hydrogen production rate is fixed at 2 kg/s, with the system aiming to minimize total power usage. The split fraction to the vent gas recycle stream is set to 0.0001 to avoid zero flows, and the cell is sized to produce 2 kg/s with an average current density of -10,000 A/m^2, allowing for a maximum current overshoot of 30%. Water conversion is constrained between 60% and 75% to optimize steam usage. In fuel cell mode, the cell operates at an average current density of 4,000 A/m^2, with an upper bound of 5,200 A/m^2. Hydrogen conversion has no specific bound due to recycling unconsumed hydrogen. Trim heaters provide 10 kW each to prevent issues with controller setpoints.

CLASSICAL PROCESS CONTROL

The SOC control system must enforce a variety of process constraints. The fuel-side inlet stream must have at least 5% (mole-basis) of hydrogen to avoid oxidation of the electrode or interconnect. The fuel-side outlet must also have at least 25% hydrogen in fuel cell mode or water in electrolysis mode to avoid cell degradation from reactant starvation. The oxygen outlet stream can have at most 35% oxygen to avoid oxidation of process equipment. The cell voltage is limited between 0.7 and 1.4 V to avoid oxidation or reduction of the cell. The maximum temperature in the cell must be kept below 1023.15 K (750 °C) to avoid degradation, and the temperature difference between the ends of the cell must be kept below 75 K to avoid thermal stress on the cell. To accomplish these goals, the following manipulated variables are used: cell potential, makeup steam/hydrogen feed rate, steam/hydrogen ratio in makeup stream, sweep feed rate, fuel trim heater duty, sweep gas trim heater duty,

fuel stream recycle ratio, sweep stream recycle ratio, and vent gas recycle ratio. Classical control uses many P and PI control loops, detailed in Table 1. Derivative action was not used, because its benefits are severely degraded by measurement noise, which cannot be added to the PETSc TS integrator used in this study for dynamic simulations with classical PI control. The PI controller model in IDAES supports both variable bounds and anti-windup, both of which were used in these simulations.

Table 1. Variable pairings for classical control.

Controller Type	Manipulated Variable (MV)	Controlled Variable (CV)
PI	Cell potential	SOC fuel outlet H_2 mole fraction
P	Makeup feed rate	Hydrogen production rate
P	Sweep feed rate	SOC stack core temperature
PI (C1I)	Steam heater duty	Steam heater outlet temperature
PI (C2I)	Sweep heater duty	Sweep heater outlet temperature
P (C1O)	Steam heater outlet temperature setpoint	SOC feed outlet temperature
P (C2O)	Sweep heater outlet temperature setpoint	SOC sweep outlet temperature
None	Feed & sweep recycle ratios, makeup H_2 & H_2O mole fractions, vent gas recycle ratio (used by NMPC, not PI)	

The cell potential has an immediate effect on the hydrogen composition of the fuel outlet stream; therefore, these two variables are paired. The makeup feed rate is then paired with the net hydrogen production/consumption rate (which can be calculated from the total current flowing through the cell, which is easily measurable). The trim heaters have an immediate impact on the stack inlet temperatures of their respective streams and are thus paired. However, it is desirable that the trim heaters also help adjust the SOC module's temperatures as needed. Therefore, a cascade arrangement is used, with another controller adjusting the inlet stream's setpoint based on the outlet stream's temperature. Typically, in cascade control, the inner controller is P and the outer controller is PI; however, an arrangement with the inner controller PI and the outer controller P was chosen to avoid controller conflicts. Finally, because the trim heaters are not engaged in SOFC mode, the sweep blower flow rate is paired with stack core temperature (measured via a thermocouple embedded in the stack) to cool the cell as needed.

NONLINEAR MODEL PREDICTIVE CONTROL

To compare the performance of classical control and advanced control strategies, an NMPC framework was developed for setpoint tracking using eight non-artificial MVs in Table 1: cell potential, makeup and sweep feed rates, feed and sweep recycle ratios, makeup H_2 and H_2O mole fractions, and vent gas recirculation (VGR) ratio. Trim heater duties are not directly tracked to enable more freedom of adjustment.

Because makeup mole fractions are tracked instead of being fixed along a linear trajectory as in the classical control case, an equality constraint pinning their sum at 0.999 is introduced to the NMPC formulation. The remainder consisted of inert gases, with fixed mole fractions of 0.0008 N_2 and 0.0002 Ar. Feed heater duty is bounded between 0 MW and 2 MW and sweep heater duty between 0 MW and 4 MW for reasonable capital equipment sizing. Condenser vapor outlet temperature is fixed at 323.15 K under the ideal condenser assumption and thus is not an MV.

$$f_{obj} = \sum_{i=0}^{N} \rho_{\mathrm{H_2}} \left(y_i - y_i^R\right)^2 + \sum_{i=0}^{N} \sum_{j \in J} \rho_j \left(u_{ij} - u_{ij}^R\right)^2 + \sum_{i=0}^{N} \sum_{k \in K} \rho'_k \left(x_{ik} - x_{ik}^R\right)^2 + \sum_{i=1}^{N} \rho' (v_i - v_{i-1})^2 + \sum_{i=0}^{N} \sum_{z=1}^{z_L} \rho_M \left(\frac{\partial T_{iz}}{\partial z \partial t}\right)^2 \quad (1)$$

As shown above, the objective function (eqn. 1) contains weighted sum of squared errors (SSE) of the trajectory-tracking of H_2 production rate as well as deviations of MVs and CVs from their reference values. A rate-of-change penalty on trim heater duties is added to attenuate oscillatory trajectories. In addition, to limit cell thermal degradation over time, the magnitude of PEN temperature curvature along the cell length (z-direction), is penalized. The first term in the objective function is the SSE of H_2 production rate, y_i, from its tracking target, y^R, at time t_i. The penalty on the H_2 rate tracking term, $\rho_{\mathrm{H_2}}$, is selected to be 1. The second term involves penalties on SSEs of the tracked MVs, u_{ij}, from their references, u^R; J represents the set of tracked MVs. Similarly, the third term penalizes deviation of the CVs (represented by set K) from their reference trajectories. The fourth term

is the rate of change penalty on trim heater duties, represented by ν. Setpoint tracking and rate of change penalty terms are scaled to be $O(1)$, and 0.01 is selected for their penalties, ρ_i, ρ_k, and ρ', to prioritize H_2 production rate tracking. The final term has a penalty of ρ_M on the sum of squares of PEN temperature curvatures in the z-direction. N is the number of steps in the prediction horizon.

For this work, it is assumed that system dynamics is unambiguously captured in the controller model; in real-world application, potential plant-model mismatch can be addressed using moving horizon estimation (MHE) with an integrating disturbance model. The controller predicts

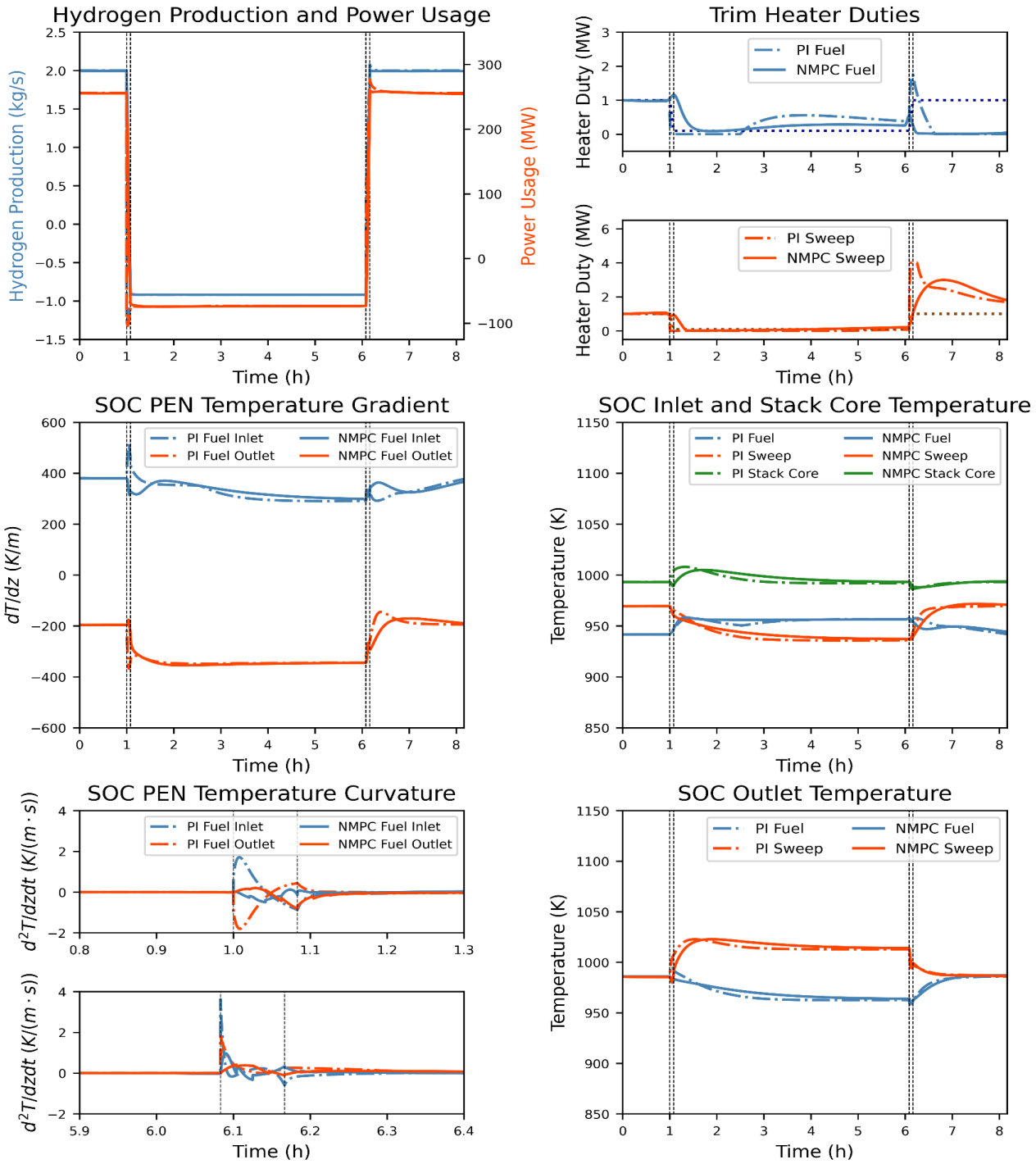

Figure 3. Comparison of classical control with NMPC in mode-switching operation.

system response for a given MV trajectory over the controller horizon with the system model and optimizes the MV trajectory for minimum objective function value. The first element of the solved trajectory is injected into the system, and the MV trajectory is re-optimized at the next sampling time over a shifted horizon. The actual decision variables in the NMPC problem are time derivatives of the MVs so that piecewise linear control profiles (first-order hold), instead of step inputs (zero-order hold), can be injected into the system. Placing a first-order hold on MVs, as opposed to a zero-order hold, smooths out the transition of control actions from the previous time step to the next and thus reduces spikiness in system response.

SIMULATION RESULTS

For performance comparison of classical control and NMPC, the SOC system was linearly ramped from maximum hydrogen production (SOEC mode) to power production (SOFC mode) and back to maximum hydrogen production in simulation. A parametric sweep on ρ_M was conducted to investigate the trade-off between operating efficiency and cell degradation, which is dependent on PEN temperature curvatures. The ramps were carried out over 5 min, with the hydrogen-power ramp followed by 5 h settling at the new operating point and the power-hydrogen ramp followed by 2 h settling. Dynamic simulations using classical process control were conducted via the IDAES interface to the PETSc [12] suite of differential algebraic equation (DAE) solvers. Because this DAE system is stiff, a variable time step implicit Euler method was used. The time step was initialized at 0.1 s, after which it typically grew to 5 s to 10 s during the initial transient after ramping started or stopped, and then to 5 min to 10 min by the end of the integration interval. When anti-reset windup was turned on or off in the PI controllers, the time step decreased to 0.5 s to 1.0 s due to the steep transition, between error integrating and not. The fully discretized control problem for NMPC had approximately 47000 equations and variables. The studies were performed on an AMD Ryzen™ 9 processor @ 3.7 GHz with 16 GB memory. On average, the solution time was 2.4 CPU s for a prediction horizon of 375 s; the problem was solved well within the sampling time of 75 s.

Figure 3 compares the performance of the two control strategies, with ρ_M set to 10^{-2} in the NMPC objective formulation; 10^{-2} offers a good balance between settling speed of hydrogen production rate, the primary output variable, and addressing thermal degradation considerations. Both classical control and NMPC reach the SOFC mode production rate of −0.92 kg/s from the SOEC mode production rate of 2.00 kg/s by the end of the five-minute ramp, with a considerable amount of overshoot observed in classical control. In the SOFC-SOEC ramp, both classical control and NMPC afford similar hydrogen production rate tracking performance, with a small amount of overshoot in the former.

Curbing temperature gradient is critical to long-term operating performance of the cell. While PEN temperature gradients are not explicitly accounted for in either classical control or NMPC, both cases are well within the safety limit of 1000 K/m, and NMPC has advantages due to smoother trajectories and lower peak magnitudes at fuel inlet and outlet.

Moreover, the time derivative of SOC PEN temperature gradient describes the trend in the gradient's temporal variation. Here, NMPC affords lower peaks in the temperature curvatures at fuel inlet and outlet, as the final term in the NMPC objective (eqn. 1) imposes squeezing action on curvatures across all z-nodes. Cell temperatures in both control strategies generally take over 2 h to settle after the ramps finish. A slightly greater overshoot is observed in sweep channel inlet temperature for NMPC after the SOFC-SOEC ramp, and the same holds for classical control stack core temperature after the SOEC-SOFC ramp. While classical control temperatures mostly settle faster than the NMPC ones, this difference is less pronounced after the SOFC-SOEC ramp. Sweep heater duty in classical control saturates at the upper bound during the SOEC-SOFC switch, whereas NMPC produces smoother profiles well within design limits. Visible deviation of trim heater duties from setpoints reveals that the system has not reached steady state even by the time of the switch back from SOFC mode to SOEC mode. Despite the different heater duty profiles by classical control and NMPC, total power usage in both strategies is similar.

CONCLUSIONS

In this work, a dynamic system flowsheet of an rSOC module and supporting auxiliary equipment was developed in the open-source, equation-based IDAES modeling framework. Control of this system for switching between maximum hydrogen production (SOEC mode) and power production (SOFC mode) was conducted with both classical control and NMPC. Dynamic simulation results show that although both control methods attain similar performance in many areas, a sophisticated classical control system involving non-intuitive cascade control arrangement was required to match the performance of NMPC in mode switching. Moreover, NMPC goes a step further by mitigating PEN temperature gradients and PEN temperature spatial-temporal derivatives along cell length more effectively than classical control does.

While classical control and NMPC attain similar total power usage in mode-switching operation, NMPC formulation in this work does not optimize for efficiency. Future work on economic MPC would allow the use of non-tracking objectives like efficiency optimization. Such

a scheme would be well suited to this rSOC system, since the system response time is slow compared to the rate at which electricity prices change. System performance while tracking more frequently alternating setpoint trajectories from fluctuating locational marginal prices (LMPs) is also critical in system economics evaluation. Another challenge is managing the trade-off between capital cost (cell degradation) and operating cost (setpoint tracking performance) over long-term operations. Finally, although the average CPU time in NMPC simulations already occupies only a small fraction of the sampling time, both advanced-step NMPC (asNMPC) and a distributed framework consisting of subsystem NMPCs can help drive down online computation delay; latency-free NMPC is a topic for further study.

ACKNOWLEDGEMENTS

This work was conducted as part of the Institute for the Design of Advanced Energy Systems (IDAES) with support from the U.S. Department of Energy's Office of Fossil Energy and Carbon Management through the Simulation-based Engineering Research Program.

This project was funded by the Department of Energy, National Energy Technology Laboratory an agency of the United States Government, through a support contract. Neither the United States Government nor any agency thereof, nor any of its employees, nor the support contractor, nor any of their employees, makes any warranty, expressor implied, or assumes any legal liability or responsibility for the accuracy, completeness, or usefulness of any information, apparatus, product, or process disclosed, or represents that its use would not infringe privately owned rights. Reference herein to any specific commercial product, process, or service by trade name, trademark, manufacturer, or otherwise does not necessarily constitute or imply its endorsement, recommendation, or favoring by the United States Government or any agency thereof. The views and opinions of authors expressed herein do not necessarily state or reflect those of the United States Government or any agency thereof.

REFERENCES

1. Ferrari ML. Advanced control approach for hybrid systems based on solid oxide fuel cells. *Applied Energy* (145): 364-373 (2015).
2. Abbaker AM, Wang H, Tian Y. Enhanced Model-Free Discrete-Time Adaptive Terminal Sliding-Mode Control for SOFC Power Plant with Input Constraints. *AJSE* 47(3): 2851-2864 (2022).
3. Botta G, Romeo M, Fernandes A, Trabucchi S, Aravind P. Dynamic modeling of reversible solid oxide cell stack and control strategy development. Energy Convers. Manag. (185): 636-653 (2019).
4. Spivey BJ, Edgar TF. Dynamic modeling, simulation, and MIMO predictive control of a tubular solid oxide fuel cell. *J Process Control* 22(8): 1502-1520 (2012).
5. Schotman R. Dynamic modelling and nonlinear model predictive control of a reversible solid oxide fuel cell: for grid-tied power tracking. Delft University of Technology (2021).
6. Xing X, Lin J, Brandon N, Banerjee A, Song Y. Time Varying Model Predictive Control of a Reversible SOC Energy-Storage Plant Based on the Linear Parameter Varying Method. *IEEE Trans on Sustain Energy* 11(3): 1589-1600 (2020).
7. Raković SV, Levine WS Handbook of Model Predictive Control. Springer International Publishing (2019).
8. Rawlings JB, Mayne DQ, Diehl MM. Model Predictive Control: Theory, Computation, and Design. Nob Hill Publishing, LLC. (2020).
9. Lee A., Ghouse JH, Eslick JE, et al., The IDAES process modeling framework and model library—Flexibility for process simulation and optimization. *J Adv Manuf Process* 3(3): e10095(2021).
10. Allan, D. A. and Eslick, J. https://github.com/IDAES/idaes-pse/blob/main/idaes/models_extra/power_generation/unit_models/soc_submodels/solid_oxide_module_simple.py.
11. Allan, Douglas, et al. "NMPC for Setpoint Tracking Operation of a Solid Oxide Electrolysis Cell System." Retrieved from: https://www.osti.gov/biblio/1964151 (2023).
12. Abhyankar S, Brown J, Constantinescu EM, Ghosh D, Smith BF, Zhang H. PETSc/TS: A Modern Scalable ODE/DAE Solver Library. *arXiv: Numer Anal* (2018).